Journal of Alloys and Compounds 509 (2011) 9589–9597

Contents lists available at ScienceDirect

Journal of Alloys and Compounds

journal homepage: www.elsevier.com/locate/jallcom

High strain rate superplasticity at intermediate temperatures of the Al 7075 alloy severely processed by equal channel angular pressing

C.M. Cepeda-Jiménez, J.M. García-Infanta, O.A. Ruano, F. Carreño*

Department of Physical Metallurgy, CENIM, CSIC, Av. Gregorio del Amo 8, 28040 Madrid, Spain

ARTICLE INFO

Article history:
Received 20 June 2011
Received in revised form 21 July 2011
Accepted 22 July 2011
Available online 28 July 2011

Keywords:
Al–Zn–Mg–Cu alloy
ECAP
Superplasticity
Deformation mechanisms
Microstructure

ABSTRACT

The mechanical properties of an overaged Al 7075-O alloy processed by ECAP were examined by tensile tests at intermediate-high temperatures ranging from 250 to 400 °C and strain rates from 10^{-5} to 10^{-1} s^{-1}. The influence of the number of ECAP passes on the ductility enhancement was evaluated. Elongation to failure, e_F, significantly increased with increasing the number of ECAP passes up to 8 at 130 °C. The alloy processed under these conditions exhibited a maximum value of 322% at 300 °C and an initial strain rate of 10^{-3} s^{-1}. High strain rate, e_F = 210%, at a strain rate as high as 10^{-2} s^{-1}. The large elongations together with lower stresses and lower stress exponents than those for the start material confirm that grain boundary sliding (GBS) is the operative deformation mechanism. A loss of superplastic behaviour at temperatures above 350 °C is related to abnormal grain growth and a change of deformation mechanism.

1. Introduction

High-strength aluminium alloys, such as the Al 7075 alloy, that combine high strength–density ratio with excellent mechanical properties are widely used for aeronautical applications [1–4]. However, this commercial alloy has only very limited formability during conventional forging at elevated temperature.

Superplastic forming (SPF) is widely used to fabricate complex parts in metallic sheets [5]. However, the expansion of SPF into the fabrication of high-volume components in the automotive and consumer product industries is currently limited because of the relatively low strain rate. Shorter forming time can provide a significant increase in economic efficiency of the SPF technique.

Accordingly, superplasticity is defined formally as the ability of a polycrystalline material to exhibit, in a generally isotropic manner, very high tensile elongations prior to failure [6]. In practice, superplastic elongations are achieved over a limited range of strain rates and temperatures [7]. Grain refining in materials results in an increase in strain rate and a decrease in the temperature at which superplasticity appears [8,9]. Therefore, several investigations have focused on optimizing grain refinement processing routes. In particular, a severe plastic deformation (SPD) technique such as equal channel angular pressing (ECAP) originally developed by Segal et al. [10,11] is an effective processing to achieve superplastic conditions [12–14]. This processing method is attractive because it has a potential for introducing very significant grain refinement into large bulk samples [15,16]. Typically, it reduces the grain size to the submicrometer level, and thereby produces materials that are capable of exhibiting unusual physical and mechanical properties [17].

The Al 7075 alloy is generally heat-treated to provide high strength at ambient temperature but in practice it is difficult to conduct ECAP processing due to the high stresses [18]. For practical applications of ECAP processing and superplastic forming of Al 7075 alloy, it appears that the best procedure for the present investigation is to process the material in an overaged condition, to subsequently superplastically form at relatively low temperatures and high strain rates, and then to apply the appropriate heat treatment to recover the optimum mechanical properties.

On the other hand, it has been reported [6,19,20] that superplasticity can be achieved in Al–Zn–Mg–Cu alloy samples subjected to ECAP. However, in all these investigations, scandium and/or zirconium additions were considered, which produce nanoscale dispersoids acting as an effective pinning agent to hinder the migration of grain boundaries [19]. Málek et al. [21,22] obtained an elongation of 200% in Al–Zn–Mg–Cu alloy without Sc or Zr additions and processed by ECAP at about 300 °C but at a relatively low strain rate of 10^{-4} s^{-1}.

The present investigation was initiated to examine the feasibility of attaining superplasticity at higher strain rate or lower temperature, through ECAP processing in an overaged Al 7075 alloy without additions of either scandium or zirconium. The purpose of this investigation is to study the intermediate-high temperature

* Corresponding author. Tel.: +34 91 5538900x217; fax: +34 91 5347425.
E-mail addresses: cm.cepeda@cenim.csic.es (C.M. Cepeda-Jiménez), carreno@cenim.csic.es (F. Carreño).

0925-8388/$ – see front matter © 2011 Elsevier B.V. All rights reserved.
doi:10.1016/j.jallcom.2011.07.076

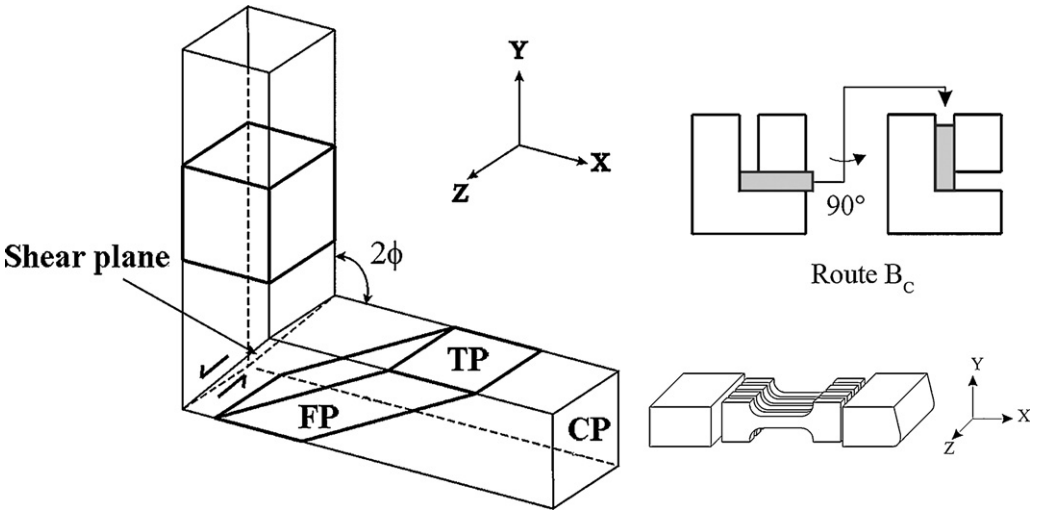

Fig. 1. Scheme of the ECAP processing of Al 7075-O samples by route B_C. The tensile samples were machined with the tensile axis parallel to the extrusion direction (*X*).

Table 1
Chemical composition of the as-received Al 7075-T651 alloy (wt%).

Si	Fe	Zn	Mg	Cu	Cr	Mn	Ti	Al
0.052	0.19	5.68	2.51	1.59	0.19	0.007	0.025	Balance

Table 2
Nomenclature used for the as-start Al 7075 alloy and ECAP processed samples.

Processing	Nomenclature
Al 7075-T651 + overaging during 5 h at 280 °C	Al 7075-O
1 pass at room temperature (T_{RT})	1p T_{RT}
1 pass at T_{RT} + 2 passes at 130 °C	3p 130 °C
1 pass at T_{RT} + 4 passes at 130 °C	5p 130 °C
1 pass at T_{RT} + 7 passes at 130 °C	8p 130 °C

behaviour of the Al 7075-O alloy processed by several conditions of ECAP processing, and to find test conditions for superplastic behaviour of this alloy.

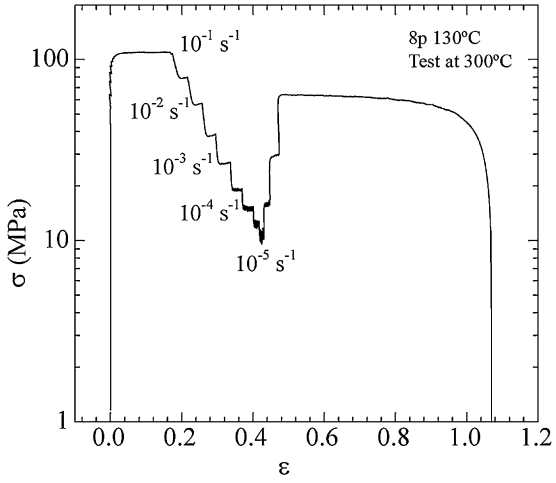

Fig. 2. Stress–strain curve obtained from a strain-rate-change test.

2. Experimental procedure

The aluminium alloy used in the present study was a rolled Al 7075-T651 plate of 12 mm in thickness. The composition in weight percentage of the alloy is included in Table 1. As-received Al 7075-T651 samples were subjected to an over-aging heat treatment at 280 °C during 5 h prior to the ECAP processing, to obtain a stable microstructure and to minimize dynamic processes, such as nucleation and precipitate coarsening during ECAP processing.

The nomenclature used for the as-start overaged Al 7075 alloy, Al 7075-O, and the ECAP processed samples is given in Table 2.

ECAP billets with dimensions 70 mm × 10 mm × 10 mm were machined along the rolling direction of the as-received plate. ECAP processing was performed using a sharp-cornered 90° ECAP die (zero die-relief angle at the outer corner of the die channel intersection), at a pressing speed of 5 mm/min. Fig. 1 shows the reference axes used in this work, where *z* is the flow plane (FP) normal, *y* the top plane (TP) normal, and *x* is the cross-section plane (CP) normal. The sense of shear on the shear plane is indicated at the die channel intersection. Samples were ECAP processed by route B_C, i.e. rotated 90° in the same sense between each pass (Fig. 1). This route was selected because it is the optimum processing procedure for attaining superplasticity in homogeneous materials [23].

The influence of the number of passes (N_p) on processing has been considered. Each sample was initially pressed once at room temperature ($N_p = 1$), and then pressed repetitively through totals of 3, 5 and 8 passes at 130 °C, equivalent to imposed strains of ~3, 5 and 8 respectively. The first pass was performed at room temperature to impose high severity to the Al 7075-O alloy and to obtain fine grain size. However, more passes at room temperature without sample cracking were not possible, and a higher processing temperature was considered to facilitate dislocation recovery and the attainment of larger accumulative strains.

The microstructure of processed samples was analyzed by transmission electron microscopy (TEM) using a JEOL JEM 2000 FX II equipment operating at 200 kV. ECAPed samples were always examined at the middle of the flow plane in order to avoid die wall effects. Grain size was measured, for all the processed conditions, from TEM images using the mean linear intercept method, without discriminating between high- and low-angle boundaries, using the Sigma Scan Pro Software. More than 300 grains for each processing condition were analyzed. Grain size data fell into log-normal distributions, so the geometric mean value was chosen as a measure of the size.

The tensile tests were performed using a universal Instron 1362 testing machine. Planar dog-bone tensile samples of 10 mm × 3 mm × 1.5 mm gauge dimensions with a radius of 3 mm were machined out from the centre portion of each ECAP-processed sample, removing 1.25 mm in thickness from each side of the sample, to avoid the non-homogeneity effect due to friction. Tensile samples were machined parallel to the flow plane (FP), in such a way that the gauge length coincided with the middle region of the ECAP samples (Fig. 1), and with the tensile axis parallel to the extrusion direction (*X*). Also, tensile samples were machined from the as-start Al 7075-O plate, being parallel to the longitudinal–transversal plane and with the tensile axis parallel to the as-received rolling direction. A set of tensile tests at elevated temperatures was performed at constant crosshead velocity, corresponding to the initial strain rate ranging between 10^{-4} s^{-1} and 10^{-1} s^{-1}. Additionally, another set of tensile tests was performed to determine the apparent stress exponent, n_{ap}, using strain-rate-change tests (SRC). Tensile samples were heated by a ellipsoidal furnace at temperatures in the range of 200–400 °C.

An example of the stress–strain rate data determination by means of SRC tests is given in Fig. 2. The initial strain rate used in these tests was 10^{-1} s^{-1}. A first strain rate jump down to 3.10^{-2} s^{-1} is performed after a plastic deformation of ~15–20%. Then, the strain rate is consecutive reduced in steps, each having $\varepsilon \sim 2$–4%, down to $\dot{\varepsilon} \sim 10^{-5}$ s^{-1}. Subsequently, the strain rate is increased in three additional steps up to 10^{-2} s^{-1}, as a check on the repeatability of flow stress measurements.

Finally, in order to investigate the deformation mechanisms, selected areas near to the failure surface were examined by electron backscatter diffraction (EBSD)

Table 3
(Sub)grain size (L_Y) measurements (nm) of the as-start Al 7075-O alloy and after ECAP processing.

Processing	L_Y (nm)
Al 7075-O	>15,000
1p T_{RT}	>400
3p 130 °C	200 ± 5
5p 130 °C	175 ± 6
8p 130 °C	163 ± 5

after the tensile tests. Orientation maps were performed in a scanning electron microscope (SEM) JEOL JSM 6500F, with a fully automatic EBSD attachment, HKL Technology, operating at an accelerating voltage and working distance of 20 kV and 15 mm, respectively. The corresponding data processing was carried out using HKL Channel 5 Software. A low angle grain boundary (LAB) was defined by a misorientation between adjacent grains of $2^\circ < \theta < 15^\circ$, and a high angle grain boundary (HAB) was defined by $\theta > 15^\circ$. HABs and LABs are shown as black and white lines respectively on the maps.

3. Results

3.1. Microstructure

Fig. 3 shows TEM micrographs corresponding to the flow plane of ECAP processed Al 7075-O samples after one pass at room temperature (Fig. 3a) and after eight passes at 130 °C (Fig. 3b). Additionally, Table 3 includes average values of the (sub)grain size (L_Y) measured from the TEM micrographs for the overaged Al 7075-O alloy after ECAP processing at 130 °C as a function of the number of passes (N_p). L_Y was the shortest length of the (sub)grain microstructure, which was perpendicular to the shear direction, because in general, the (sub)grain shape was slightly elongated in the shear direction of the last ECAP pass.

The as-start Al 7075-O alloy after overaging treatment showed large grains that were elongated and flattened parallel to the rolling direction. The average grain thickness and length in the rolling direction (RD) were about 15 and 350 μm respectively. After one pass at room temperature (Fig. 3a) the (sub)grain size decreases to ~400 nm. A high density of dislocations is retained and the grain boundaries are wavy and ill-defined. The use of the room temperature for the first pass suppresses dynamic recovery, allowing the density of the accumulated dislocations to reach a higher level than that achievable at higher temperature.

A nearly equiaxed (sub)grain structure after eight ECAP passes (Fig. 3b) has replaced the bandlike substructure formed in the initial pressing operation, although (sub)grains aligned in the shear direction of the last pass can still be observed. There was generally a lower density of intragranular dislocations with an increase in the number of ECAP passes (N_p). The increase in N_p at 130 °C allowed to achieve a (sub)grain size of ~163 nm for the sample processed by eight passes at 130 °C (Fig. 3b and Table 3). The most important change observed with increasing strain was the decrease of both the width and the length of the (sub)grains, rapidly for the initial strains (one pass), and more slowly at higher strain levels (Table 3). In addition, as shown in a previous work [24] where grain-boundary misorientation distributions corresponding to Al 7075-O alloy samples subjected to 3 and 8 ECAP passes at 130 °C were measured, the fraction of high-angle grain boundaries (f_{HAB}) increased from 37% after 3 passes ($\varepsilon \sim 3$) to 56% after 8 passes ($\varepsilon \sim 8$).

Another feature revealed in the TEM micrographs of Fig. 3 is a large number of fine bright particles distributed through the grains, which are indicated by black arrows. These spherical precipitates ($Mg(Zn_2,AlCu)$ and $Al_{18}Mg_3Cr_2$) coarsened during the previous overaging treatment but remained unaffected by ECAP processing, with sizes similar to those of the initial overaged state, ranging from ~100 to ~200 nm.

3.2. Tensile tests at constant strain rate

Plots of true stress against true strain (σ–ε curves) are shown in Fig. 4 for samples tested in tension at different temperatures (250–400 °C) and strain rates (10^{-1}–10^{-4} s^{-1}). In Fig. 4a results are given for the as-start Al 7075-O alloy samples, whereas in Fig. 4b the curves relate to tests conducted for the ECAPed Al 7075-O alloy processed by the optimum condition of 8 passes at 130 °C. Each strain rate is represented by a symbol and a colour that will appear in gray in a printed version of this paper. In addition, the dependence of strain rate and temperature on the elongation to failure (e_F) as a function of the number of passes (N_p) has been included in Table 4.

It is shown for the as-start 7075-O alloy (Fig. 4a), that at a given strain rate, the increase in test temperature produces a decrease in σ and an increase in ε_F.

On the other hand, for the ECAPed sample by 8p at 130 °C (Fig. 4b), similar trend on stress decrease and ductility enhancement with test temperature is observed only up to 300 °C, where a maximum ductility of $\varepsilon_F = 1.44$ ($e_F = 322\%$) at $\dot{\varepsilon} = 10^{-3}$ s^{-1} has been achieved. However, an important decrease in ductility at 350 °C for all strain rates can be observed, being $\varepsilon_F = 0.72$ ($e_F = 105\%$) at $\dot{\varepsilon} = 10^{-3}$ s^{-1}. This value is very similar to that for the as-start Al 7075-O alloy under the same test conditions (Fig. 4a).

It should be noted that the flow stress for the ECAPed material (Fig. 4b) falls below that of the un-pressed material at all temperatures, especially at the two lower strain rates (Fig. 4a). In addition, the ductility of the processed material is much higher. The lower stresses and higher ductilities obtained for the ECAP processed sample, in comparison with those for the as-start material, are due to its finer grain size as a result of the processing.

The influence of the number of ECAP passes at 130 °C on the elongation to failure between 250 and 350 °C can be analyzed in Table 4. In general, it is observed that for a given test temperature and strain rate, the ductility increases with N_p. The ECAPed Al 7075-O by 1 pass at room temperature shows higher ductility than that for the as-start Al 7075-O alloy at 300 and 350 °C. Additionally, the increase in the number of ECAP passes up to 5 passes enhances the ductility above $e_F = 200\%$. This suggests that from 5 ECAP passes, the ECAPed Al 7075-O alloy exhibits superplasticity, even at a low temperature of 250 °C ($e_F = 239\%$). At 300 °C, a ductility of 271% was obtained at a strain rate of 10^{-3} s^{-1} after 5 ECAP passes at 130 °C. However, the maximum ductility of 322% was achieved at a temperature of 300 °C and strain rate of 10^{-3} s^{-1} after 8 ECAP passes at 130 °C (Table 4). Other noteworthy e_F values obtained after 8 ECAP passes at 130 °C are: $e_F = 210\%$ at 300 °C and $\dot{\varepsilon} = 10^{-2}$ s^{-1} and $e_F = 217\%$ at 250 °C and $\dot{\varepsilon} = 10^{-3}$ s^{-1}. However, at 350 °C, the elongations dropped drastically and were consistently lower than 190% at all strain rates and N_p.

3.3. Tensile tests with strain-rate-changes

In order to characterize the creep behaviour of the as-start Al 7075-O alloy and ECAPed samples, strain rate-flow stress data at different temperatures (200–400 °C) were obtained during SRC tests, as shown in Fig. 2. The data presented from SRC tests correspond to steady-state behaviour, where flow stress is measured after stabilizing at a new strain rate. Strain-rate-change tests in the steady state enables the attainment of several data pairs by using only one test sample as detailed elsewhere [25]. The logarithm of the strain rate, $\dot{\varepsilon}$, is represented as a function of logarithm of the true flow stress, σ, in Fig. 5 for the as-start Al 7075-O alloy and ECAPed-8p-130 °C sample. Separated graphs corresponding to different test temperatures are given.

Table 4
Elongation to failure (e_F, in percent) obtained from tensile tests at constant strain rate ($\dot{\varepsilon} = cte$) for the as-start Al 7075-O alloy, and after ECAP processing as a function of the number of passes at 130 °C.

T (°C)	$\dot{\varepsilon}$ (s^{-1})	Al 7075-O (%)	1p-T_{RT} (%)	3p-130 °C (%)	5p-130 °C (%)	8p-130 °C (%)
250	10^{-1}	63	38	53	53	100
	10^{-2}	62	50	77	100	134
	10^{-3}	64	66	140	157	217
	10^{-4}	–	74	127	239	237
300	10^{-1}	73	67	80	107	122
	10^{-2}	72	71	116	166	210
	10^{-3}	85	100	188	271	322
	10^{-4}	–	109	177	226	242
350	10^{-1}	88	90	123	138	98
	10^{-2}	97	115	154	191	121
	10^{-3}	91	143	121	171	105

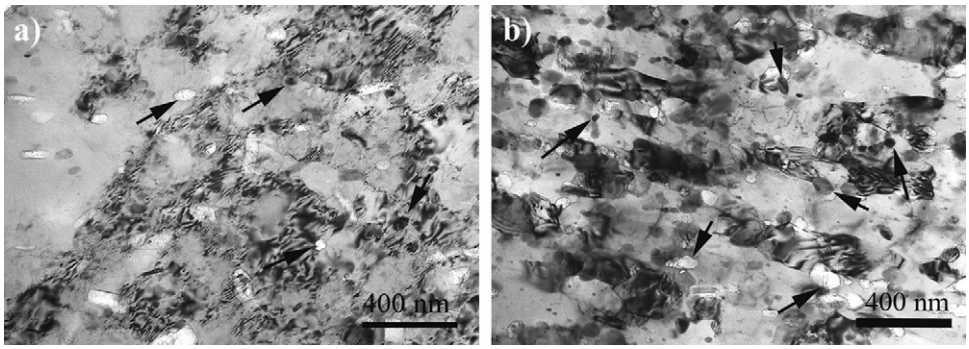

Fig. 3. TEM micrographs showing the microstructure of the Al 7075-O alloy after two conditions of ECAP processing: (a) 1p-T_{RT}; (b) 8p-130 °C. The black arrows in the micrographs show the location of some precipitates.

The experimental data points at the same temperature are joined by a line. The apparent stress exponent, n_{ap}, is directly obtained from the slope of this line using the relation (1):

$$n_{ap} = \left.\frac{\partial \ln \dot{\varepsilon}}{\partial \ln \sigma}\right|_T \quad (1)$$

Accordingly, the minimum apparent stress exponent calculated for each sample and test temperature has been included in each graph in Fig. 5.

In addition, the black colour open symbols correspond to $\dot{\varepsilon} - \sigma$ pairs obtained by decreasing strain-rate steps, and the red colour filled symbols represent these obtained by increasing steps from $\dot{\varepsilon} = 10^{-5}$ to $\dot{\varepsilon} = 10^{-2}\ s^{-1}$. (For interpretation of the references to colour in this text, the reader is referred to the web version of this article).

It is apparent that the samples processed by ECAP exhibit lower flow stresses in these plots with respect to the as-start Al 7075-O alloy except only when testing at the highest strain rates at 200 and 250 °C, and at the highest temperature of 400 °C. Furthermore, the $\dot{\varepsilon} - \sigma$ curves for the ECAPed-8p-130 °C sample strongly shift toward lower stress values with increasing temperature up to 350 °C. However, the $\dot{\varepsilon} - \sigma$ curves for processed and as-start samples practically coincide at 400 °C. In addition, both the samples processed by ECAP and the as-start material show similar values of $n_{ap} = 5$–6 when testing at 400 °C, and the minimum values are obtained for low strain rates. This value of n_{ap} is consistent with dislocation glide as the rate-controlling flow process [26].

Additionally, the ECAP processed samples (8p-130 °C) show values of n_{ap} lower than those for the as-start Al 7075-O alloy up to $T = 350$ °C. While the minimum value of n_{ap} for the as-start material is observed for the lowest strain rates at all test temperatures considered, for the processed samples the minimum value of n_{ap} is generally registered at strain rates between $10^{-3}\ s^{-1}$ and $10^{-2}\ s^{-1}$. For the ECAPed sample, n_{ap} varies with testing temperature in the range $n_{ap} = 3.2$–5, and for the as-start alloy it is ranged between 6 and 13. The minimum $n_{ap} \sim 3.2$ for the ECAPed-8p-130 °C material occurs at 300 °C. A low stress (σ) and an elongation >200% together with low n values has been considered to be an indicator of the appearance of superplasticity and grain boundary sliding mechanism [27].

On the other hand, $\dot{\varepsilon} - \sigma$ pairs corresponding to increasing strain-rate steps (filled symbols in Fig. 5) for the as-start material perfectly coincide with $\dot{\varepsilon} - \sigma$ pairs corresponding to the decreasing steps. This does not occur for the ECAPed sample up to $T = 350$ °C, and the $\dot{\varepsilon} - \sigma$ pairs corresponding to the increasing steps systematically are shifted to higher stress values. At 400 °C, the $\dot{\varepsilon} - \sigma$ pairs for increasing and decreasing steps coincide, likewise than those for the as-start Al 7075-O alloy. It is worth noting that during the increasing strain-rate-changes, the sample accumulates approximately 45 min more at the test temperature, than during the decreasing steps, and grain coarsening may occur. This information is very useful to determine the deformation mechanisms operating at high temperature, because GBS depends on grain size.

In Fig. 6, the strain rate against the flow stress from SRC tests has been plotted for the as-start Al 7075-O alloy, and after ECAP processing as a function of the number of passes at 130 °C. Furthermore, the upper graph in Fig. 6 corresponds to SRC tests carried out at 250 °C, and the lower graph gives the results obtained at 300 °C.

The $\dot{\varepsilon} - \sigma$ curves shift to lower creep stress with the increase in the number of ECAP passes (N_p) with respect to the as-start material, for both test temperatures (Fig. 6). This effect is very important at low $\dot{\varepsilon}$, being the creep stress for the ECAPed-8p-130 °C Al 7075-O alloy four times lower than that for the as-start alloy. In addition, whereas the as-start material again exhibits a stress exponent $n_{ap} \sim 8$–13 over the range of strain rates considered, the results from the samples processed by ECAP present lower n_{ap} values for higher N_p at increasing $\dot{\varepsilon}$.

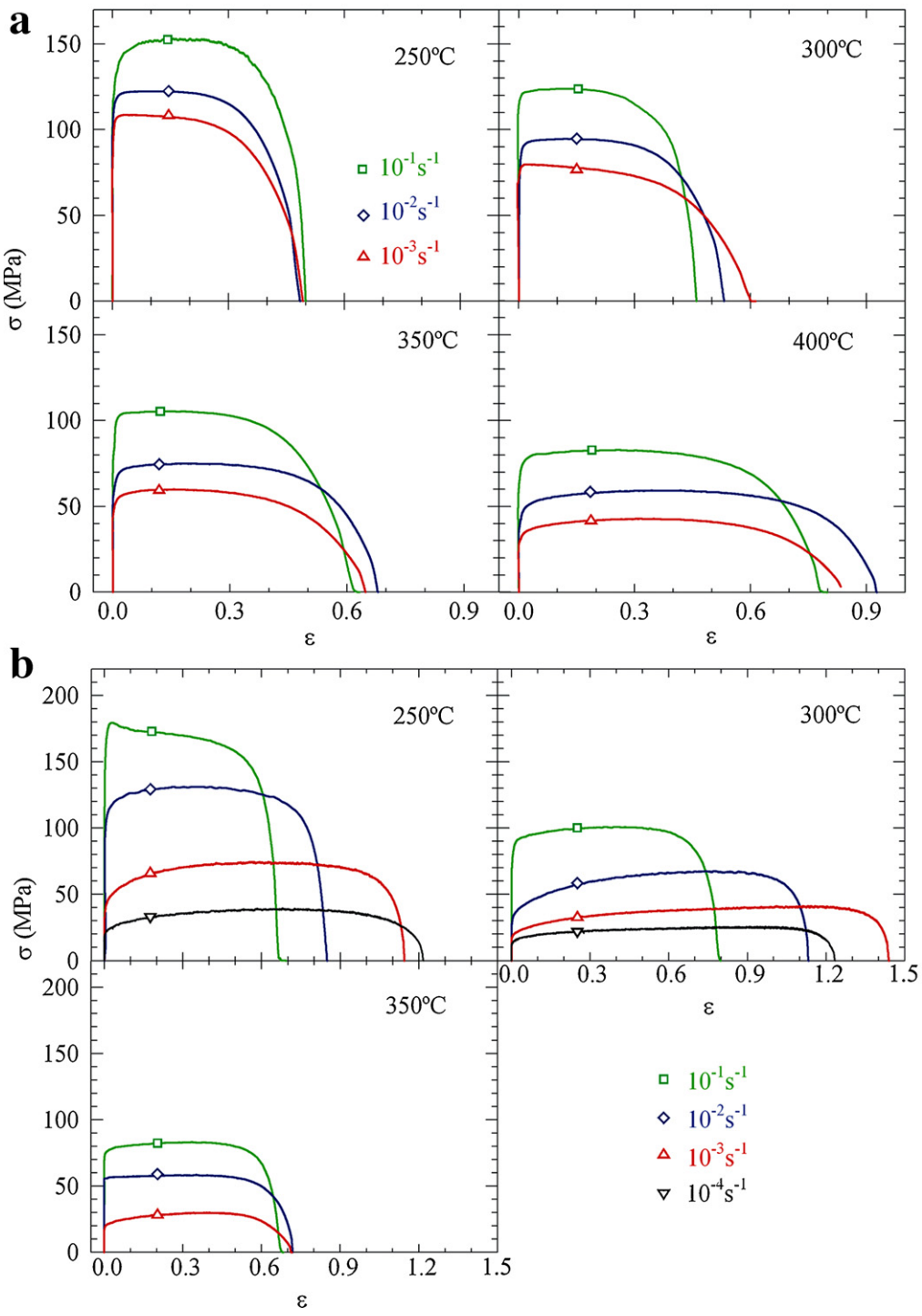

Fig. 4. Stress–strain curves obtained from tensile tests at constant strain-rate at different temperatures for (a) the as-start Al 7075-O alloy and (b) after 8 ECAP passes at 130 °C.

Fig. 7 shows orientation maps obtained from the EBSD technique for the gauge section of the Al 7075-O alloy processed through eight ECAP passes at 130 °C, and then subjected to SRC tests at 300 °C (Fig. 7a), 350 °C (Fig. 7b) and 400 °C (Fig. 7c). It is worth noting that deformation during the SRC tests was carried out mostly at $10^{-2}\,s^{-1}$ according to Fig. 2. The EBSD maps have been colour coded according to the inverse pole figure (IPF) shown in the inset, and the colours represent the crystallographic orientations parallel to the *Z* axis.

It is apparent from Fig. 7 that the grains remain fairly equiaxed after tensile testing at 300 °C (Fig. 7a), although coarsen slightly, and show some visible elongation along the tensile axis at 350 °C (Fig. 7b). An abnormal coarsening is observed after testing at 400 °C (Fig. 7c). Nearly all grain boundaries show high-angle misorientation in the samples tested at 300 and 350 °C (Fig. 7a and b). The average grain size is approximately 2 and 3.8 μm after testing at 300 and 350 °C respectively, and the grain shape does not correlate directly with the great elongation experimented by these samples.

On the contrary, the ECAPed-8p-130 °C sample tensile tested at 400 °C (Fig. 7c) presents coarsened grains, with sizes higher than 25 μm, which are very elongated in the tensile direction. These

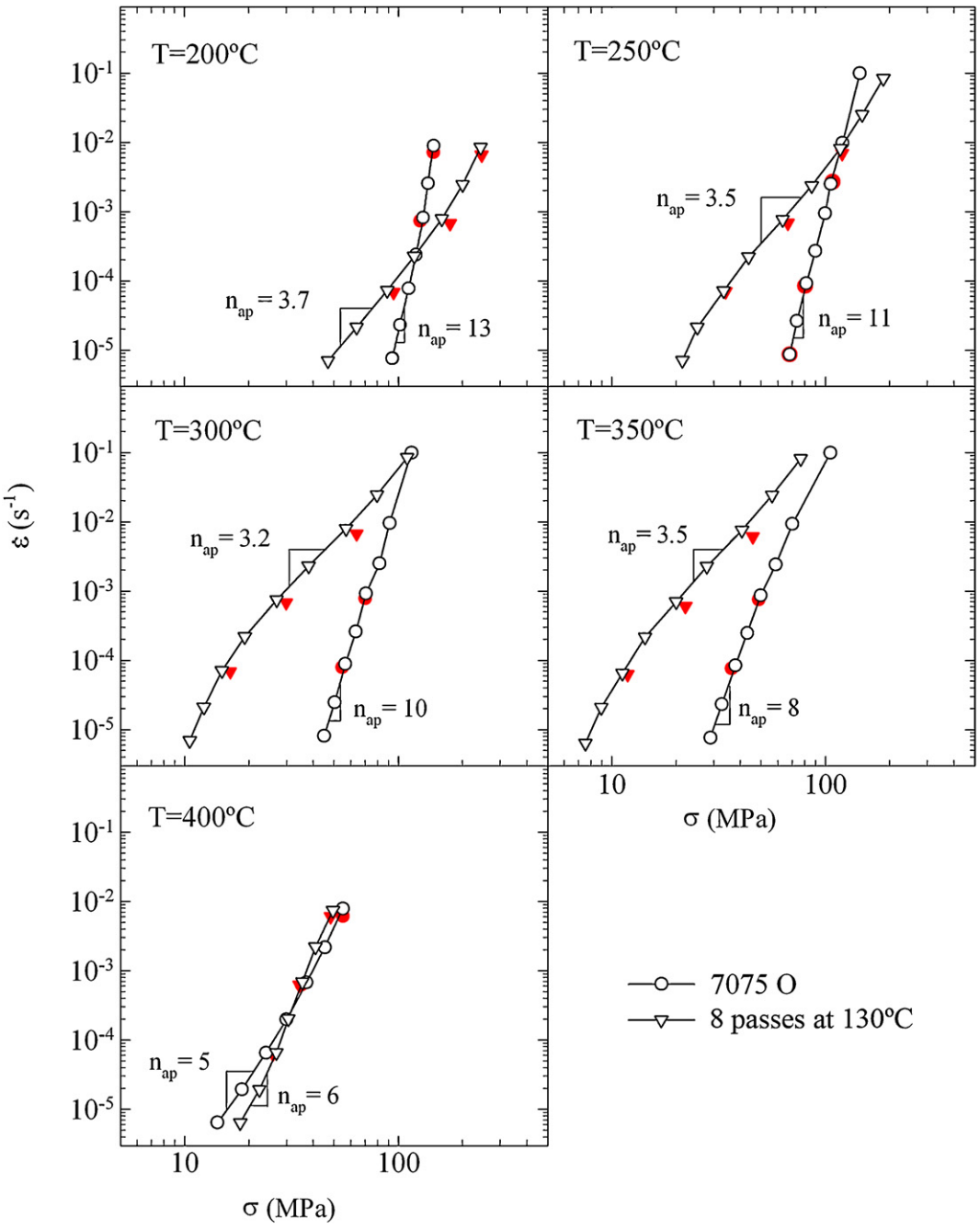

Fig. 5. Strain rate–stress curves at various temperatures (200–400 °C) for the as-start Al 7075-O alloy and after 8 passes of ECAP processing at 130 °C.

observations have significance regarding the deformation mechanisms, which are discussed below.

4. Discussion

The mechanical properties at intermediate-high temperature of an overaged Al 7075-O alloy processed by ECAP have been examined by tensile tests at temperatures ranging from 200 to 400 °C, and strain rates ranging from 10^{-5} to 10^{-1} s^{-1}.

A refined microstructure with an average grain size of ~163 nm was obtained after ECAP processing through 8 passes at 130 °C (Table 3 and Fig. 3). This material processed under this ECAP condition exhibited a maximum elongation to failure of ~322% at a temperature of 300 °C, and an initial strain rate of 10^{-3} s^{-1}. A superplastic elongation of ~210% was recorded at a strain rate as high as 10^{-2} s^{-1} (Table 4). High-strain rate superplasticity (HSR SP) is generally defined as the occurrence of superplastic ductility at strain rates at and above 10^{-2} s^{-1} [28]. It is apparent therefore, that HSR SP was achieved in the present study for the Al 7075-O alloy by ECAP processing under determined conditions. Furthermore, superplastic elongations at lower temperature or higher strain rate than those reported up to date for this commercial Al 7075 alloy without the addition of Sc or Zr have been achieved.

This work establishes ECAP as a viable processing for achieving the ultrafine-grained microstructure, which is an important prerequisite in order to attain superplasticity at high strain rate. Nevertheless, the introduction of an extremely fine grain size through ECAP is not a sufficient criterion to achieve superplastic forming because it is necessary also that the grains remain reasonably stable at high temperature. This difficulty was overcome

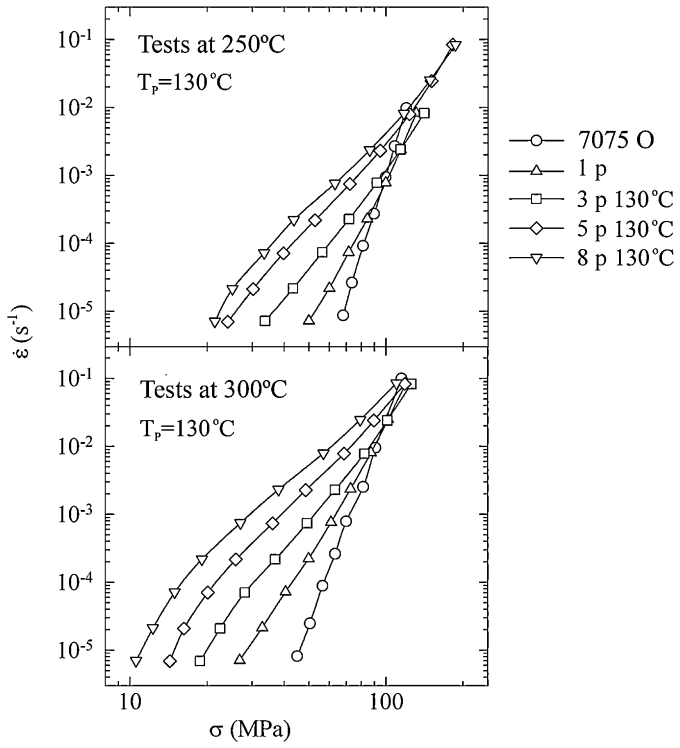

Fig. 6. Strain rate–stress curves for the as-start Al 7075-O alloy and after one ECAP pass at room temperature or different number of ECAP passes at 130 °C. The upper graph corresponds to strain-rate-change tests carried out at 250 °C and the lower graph to those performed at 300 °C.

in the present investigation because grain growth is restricted in the Al 7075-O alloy through the presence of relatively fine precipitates, 100–200 nm in size (Fig. 3), which remain stable at the high temperatures required for superplastic flow. The presence of these particles is very effective in restricting grain growth so that fine grains are retained at elevated temperatures up to at least ~350 °C (Fig. 7).

Since all of the samples processed by ECAP achieved a large refinement in grain size (Table 3), between ~400 nm after 1p at room temperature and ~163 nm for 8p at 130 °C, the important variations in the measured elongations cannot be attributed only to the grain size. It is well known that very fine subgrains are usually formed during the first pass, and the following passes result in an increase in the boundary misorientation [29]. Thus, the difference in ductility between different ECAP conditions arises because of the nature of the grain boundary misorientations. It is apparent in Table 4 that the maximum elongation is displaced to higher strain rates or lower test temperatures when the number of ECAP passes increases up to 8. This is attributed to the increasing fraction of high-angle boundaries with increasing numbers of passes, i.e. with accumulated strain, being f_{HAB} = 37% after 3 passes ($\varepsilon \sim 3$) and 56% after 8 passes ($\varepsilon \sim 8$) [24].

In order to examine the rate-controlling flow mechanism, the initial strain rate was plotted logarithmically against the flow stress for the as-start Al 7075-O alloy, and each ECAPed sample SRC tested at different temperatures (Figs. 5 and 6), where the slope of each line delineates the stress exponent, n_{ap}.

The high n_{ap} values observed for the as-start Al 7075-O alloy (Fig. 5) together with the presence of the precipitates in the initial overaged state gives microstructural basis for the use of Sherby substructure constant model [30]. This model predicts n = 8 and a dependence of the strain rate with the interparticle distance, λ, since the subgrain size is constant (not being a function of stress). The as-start Al 7075-O alloy should creep under constant microstructure conditions due to the amount of particles present in the microstructure. However, particle coarsening strongly depends on applied strain rates because the time of testing can be dramatically different. At low applied strain rates, long testing times are needed to measure steady state stresses, whereas much shorter times are needed at high applied strain rates. Consequently, high applied strain rates imply short time at high temperature and, generally, only a small increase in inter-particle distance occurs during testing. On the contrary, at low stresses, long time at high temperature allows the formation of coarsened particles, determining a larger increase of inter-particle distance during testing. In addition, power law breakdown occurs at intermediate temperatures (~200–250 °C). Therefore, the relationship between λ and σ justifies the creep behaviour of this alloy with stress exponents ranged between n_{ap} = 5 and 13.

For the ECAPed-8p-130 °C sample, much lower stresses, ductility values higher than 200% and stress exponents (n_{ap}) close to 3 suggest a transition to grain-boundary-sliding creep mechanism (GBS), operating already at 250 °C (Fig. 5). At 300 °C, the minimum value, n_{ap} = 3.2, at the strain rate of 10^{-3}–10^{-2} s^{-1} was measured. In addition, n_{ap} = 3.7 was achieved at 10^{-4}–10^{-5} s^{-1} and 200 °C, indicating that low-strain rate superplasticity was developed at this temperature in the ECAPed Al 7075-O alloy. On the contrary, at 400 °C, the stress values become similar to those of the as-start material, and the n_{ap} values were consistently higher than 5 for various strain rates, indicating again a change in mechanism. The higher n_{ap} values justify also the lower elongation in the ECAPed sample above 350 °C (Table 4).

In Fig. 7a and b, the grains are fairly equiaxed in the gauge length in spite of the large elongations achieved both for the ECAPed-8p-130 °C sample tested at 300 and 350 °C, with average sizes of ~2 and ~3.8 μm, respectively. This grain size measured by EBSD is coarser than that measured by TEM for the as-processed sample (Fig. 3 and Table 3). However, from a superplasticity point of view, an 8 μm grain size is still considered to be fine for aluminium alloys [31]. Thus, as in normal superplasticity, grain growth occurs during superplastic deformation within the gauge length [32], and justifies the observed n_{ap} values higher than 2. In addition, significant texture randomization has taken place during the tensile tests. The decrease in the texture intensity during superplastic deformation is consistent, and again corroborates, the operation of GBS mechanism that implies multiple grain rotation [33].

On the contrary, when tested at 400 °C, the ECAPed sample displayed a duplex microstructure (Fig. 7c), with a small number of large grains being surrounded by arrays of fine grains, indicating the occurrence of abnormal grain growth. At 400 °C extensive precipitate dissolution and coarsening takes place, especially for Mg and Zn rich precipitates, thus decreasing their pinning effect on the grain boundaries. The new grains grow rapidly, producing a heterogeneous microstructure and consequently a premature failure of the material. Grain size coarsening produced during heating to the test temperature and during the tensile test leads to a transition between GBS and dislocation-dominated flow, increasing the stress exponent (Fig. 5).

4.1. Temperature interval to obtain superplasticity in the ECAPed Al 7075-O alloy

The objective of this study was to analyze the feasibility of attaining superplasticity in the overaged Al 7075-O alloy at higher strain rates or lower temperatures than those reported up to date. This objective has been achieved especially after ECAP processing through 8 passes at 130 °C, and under different test conditions. Accordingly, Fig. 8 plots the variation of the elongation to failure (e_F) against the initial strain rate for the as-start Al 7075-O alloy, and

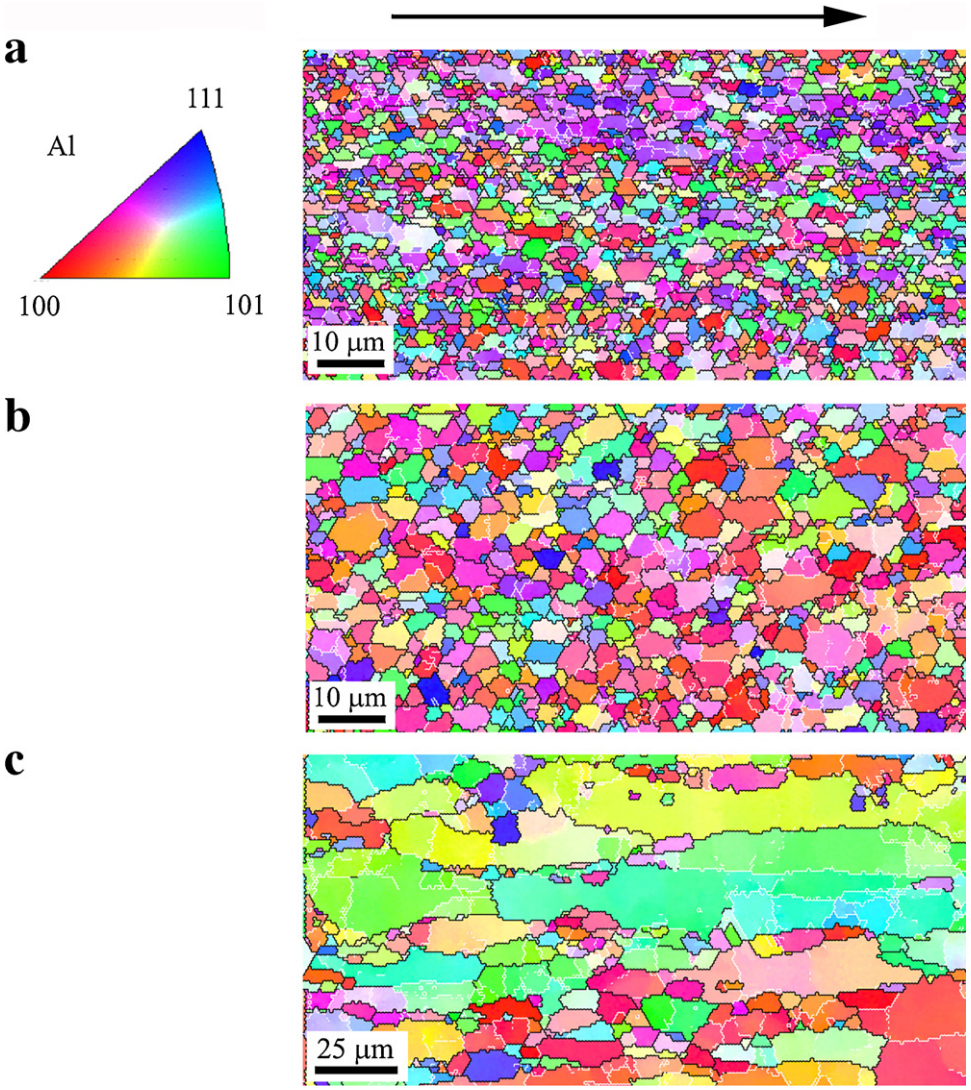

Fig. 7. EBSD maps of the deformed region of ECAPed-8p-130 °C Al 7075-O samples. The strain-rate-change tests were carried out at (a) 300 °C, (b) 350 °C and (c) 400 °C. The tensile direction is indicated by the horizontal arrow.

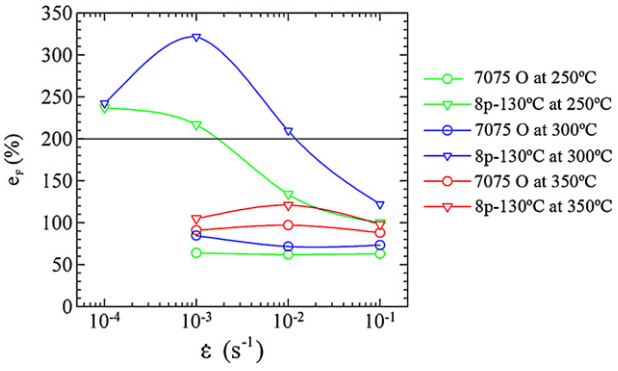

Fig. 8. Elongation to failure versus strain rate curves for the as-start Al 7075-O alloy and after 8 ECAP passes at 130 °C. Data were obtained from tensile tests carried out at constant strain rate at 250, 300 and 350 °C.

the optimum ECAPed-8p-130 °C sample tensile tested between 250 and 350 °C. A horizontal line has been traced at e_F = 200% to delimit the elongation above which superplasticity is usually accepted. Thus, it is possible to delimit the interval T_{min}–T_{max} where this superplasticity criterion is fulfilled. It is apparent that the as-start material exhibits elongations much lower than 200% over the entire strain rate range from 10^{-4} to 10 s^{-1}. On the other hand, at test temperatures between 250 and 300 °C, the ECAPed-8p-130 °C Al 7075-O sample was considerably more ductile than the as-start material. It should be noted that elongations higher than 200% are obtained at 250 °C (Fig. 8), temperature that can be considered low for aluminium alloys. On the contrary, the ECAPed-8p-130 °C samples tensile tested at 350 °C showed much lower ductility than that for samples tested at 300 °C, being the ductility values very similar to those for the as-start Al 7075-O alloy. Therefore, the ductility enhancement of the ECAPed alloy is lost at 350 °C (0.65 T_f). This result establishes an upper limit (T_{max}) at 350 °C, above which the ECAPed-8p-130 °C sample presents similar mechanical behaviour than that for the as-start Al 7075-O alloy. Likewise, elongation to failure values higher than 200% were observed for Al 7075-O samples processed by 5 passes at 130 °C (Table 4), which were tensile tested at 250 and 300 °C. However, e_F > 200% was not observed by tensile test at 350 °C for this ECAP processing condition, indicating that a critical temperature exists, at which abnormal grain growth takes place.

On the other hand, from the tensile tests performed at 250 °C, elongations higher than 200% were observed only at intermediate

strain rates ($\leq 10^{-3}$) (Table 4). This temperature, therefore, can be considered as the lower limit for obtaining superplastic properties.

In summary, grain boundary sliding and high strain rate superplasticity may be achieved in the commercial Al 7075 alloy from an initial overaged state and processed through 8 ECAP passes at 130 °C.

5. Conclusions

An overaged Al 7075-O alloy was successfully processed by different number of ECAP passes at 130 °C, and its mechanical properties at intermediate-high temperatures were analyzed. The main conclusions of this study are as follows:

1. The grain size, its misorientation and stability at elevated temperatures were found to play a decisive role in the deformation behaviour of the ECAPed Al 7075-O alloy. Fine and highly misoriented grain sizes in the processed material lead to lower stresses, higher ductility and lower stress exponents than those for the start material.
2. The maximum elongation to failure of 322% was obtained for ECAPed samples by 8 passes at 130 °C, which were tensile tested at 300 °C and $10^{-3}\ s^{-1}$. Furthermore, an elongation of 210% appears at strain rate as high as $10^{-2}\ s^{-1}$, indicating that high strain rate superplasticity was achieved.
3. An interval T_{min}–T_{max}, 250–350 °C, where the ECAPed Al 7075-O alloy shows high ductility has been determined.
4. Up to 300 °C the ultrafine grain sizes introduced by ECAP are exceptionally stable because of the presence of a reasonably homogeneous distribution of $Mg(Zn_2,AlCu)$ and $Al_{18}Mg_3Cr_2$ precipitates. On the contrary, above 350 °C, abnormal grain growth larger than 25 μm was observed, because of partial precipitates dissolution.
5. Grain boundary sliding is the main deformation mechanism at the maximum superplasticity conditions in the ECAPed Al 7075-O alloy, as confirmed by EBSD with the presence of equiaxed grains and random texture.

Acknowledgement

Financial support from MICINN (Project MAT2009-14452) is gratefully acknowledged.

References

[1] A. Deschamps, Y. Bréchet, Mater. Sci. Eng. A251 (1998) 200–207.
[2] C.M. Cepeda-Jiménez, M. Pozuelo, J.M. García-Infanta, O.A. Ruano, F. Carreño, Metall. Mater. Trans. A 40 (2009) 69–79.
[3] C.M. Cepeda-Jiménez, J.M. García-Infanta, M. Pozuelo, O.A. Ruano, F. Carreño, Scr. Mater. 61 (2009) 407–410.
[4] R. Jayaganthan, H.-G. Brokmeier, B. Schwebke, S.K. Panigrahi, J. Alloys Compd. 496 (2010) 183–188.
[5] K. Wang, F.C. Liu, Z.Y. Ma, F.C. Zhang, Scr. Mater. 64 (2011) 572–575.
[6] C. Xu, M. Furukawa, Z. Horita, T.G. Langdon, Acta Mater. 51 (2003) 6139–6149.
[7] T.G. Langdon, Mater. Sci. Eng. A 137 (1991) 1–11.
[8] R.Z. Valiev, D.A. Salimonenko, N.K. Tsenev, P.B. Berbon, T.G. Langdon, Scr. Mater. 37 (1997) 1945–1950.
[9] N. Tsuji, K. Shiotsuki, Y. Saito, Mater. Trans. 40 (1999) 765–771.
[10] V.M. Segal, Mater. Sci. Eng. A 197 (1995) 157–164.
[11] S. Ferrasse, V.M. Segal, K.T.H. Hartwig, R.E. Goforth, J. Mater. Res. 12 (1997) 1253–1261.
[12] M. Mabuchi, K. Ameyama, H. Iwasaki, K. Higashi, Acta Mater. 47 (1999) 2047–2057.
[13] W.J. Kim, C.W. An, Y.S. Kim, S.I. Hong, Scr. Mater. 47 (2002) 39–44.
[14] K. Matsubara, Y. Miyahara, Z. Horita, T.G. Langdon, Acta Mater. 51 (2003) 3073–3084.
[15] S. Lee, M. Furukawa, Z. Horita, T.G. Langdon, Mater. Sci. Eng. A 342 (2003) 294–301.
[16] T. Grosdidier, D. Goran, G. Ji, N. Llorca, J. Alloys Compd. 504S (2010) S456–S459.
[17] R.Z. Valiev, R.K. Islamgaliev, I.V. Alexandrov, Prog. Mater. Sci. 45 (2000) 103–189.
[18] M.R. Roshan, S.A. Jenabali-Jahromi, R. Ebrahimi, J. Alloys Compd. 509 (2011) 7833–7839.
[19] I. Nikulin, R. Kaibyshev, T. Sakai, Mater. Sci. Eng. A 407 (2005) 62–70.
[20] C. Xu, M. Furukawa, Z. Horita, T.G. Langdon, Acta Mater. 53 (2005) 749–758.
[21] P. Málek, M. Cieslar, Mater. Sci. Eng. A 324 (2002) 90–95.
[22] P. Málek, M. Cieslar, R.K. Islamgaliev, J. Alloys Compd. 378 (2004) 237–241.
[23] S. Komura, M. Furukawa, Z. Horita, M. Nemoto, T.G. Langdon, Mater. Sci. Eng. A 297 (2001) 111–118.
[24] C.M. Cepeda-Jiménez, J.M. García-Infanta, O.A. Ruano, F. Carreño, J. Alloys Compd. 509 (2011) 8650–8657, doi:10.1016/j.jalcom.2011.06.070.
[25] F. Carreño, O.A. Ruano, Acta Mater. 46 (1998) 159–167.
[26] O.D. Sherby, P.M. Burke, Prog. Mater. Sci. 13 (1968) 323–390.
[27] O.A. Ruano, O.D. Sherby, Rev. Phys. Appl. 23 (1988) 625–637.
[28] K. Higashi, M. Mabuchi, T.G. Langdon, ISIJ Int. 36 (1996) 1423–1438.
[29] Z. Horita, T. Fujinami, M. Nemoto, T.G. Langdon, Metall. Mater. Trans. A 31 (2000) 691–701.
[30] O.D. Sherby, R.H. Klundt, A.K. Miller, Metall. Trans. A 8 (1977) 843–850.
[31] T.G. Nieh, L.M. Hsiung, J. Wadsworth, R. Kaibyshev, Acta Mater. 46 (1998) 2789–2800.
[32] S. Lee, P.B. Berbon, M. Furukawa, Z. Horita, M. Nemoto, N.K. Tsenev, R.Z. Valiev, T.G. Langdon, Mater. Sci. Eng. A 272 (1999) 63–72.
[33] J.A. del Valle, M.T. Pérez-Prado, O.A. Ruano, J. Eur. Ceram. Soc. 27 (2007) 3385–3390.